Elevated energy requirement of cone photoreceptors

Norianne T. Ingram[a,b], Gordon L. Fain[a,b], and Alapakkam P. Sampath[b,1]

[a]Department of Integrative Biology and Physiology, University of California, Los Angeles, CA 90095-7239; and [b]Department of Ophthalmology, Jules Stein Eye Institute, University of California, Los Angeles, CA 90095-7000

Edited by King-Wai Yau, Johns Hopkins University School of Medicine, Baltimore, MD, and approved July 6, 2020 (received for review January 29, 2020)

We have used recent measurements of mammalian cone light responses and voltage-gated currents to calculate cone ATP utilization and compare it to that of rods. The largest expenditure of ATP results from ion transport, particularly from removal of Na^+ entering outer segment light-dependent channels and inner segment hyperpolarization-activated cyclic nucleotide-gated channels, and from ATP-dependent pumping of Ca^{2+} entering voltage-gated channels at the synaptic terminal. Single cones expend nearly twice as much energy as single rods in darkness, largely because they make more synapses with second-order retinal cells and thus must extrude more Ca^{2+}. In daylight, cone ATP utilization per cell remains high because cones never remain saturated and must continue to export Na^+ and synaptic Ca^{2+} even in bright illumination. In mouse and human retina, rods greatly outnumber cones and consume more energy overall even in background light. In primates, however, the high density of cones in the fovea produces a pronounced peak of ATP utilization, which becomes particularly prominent in daylight and may make this part of the retina especially sensitive to changes in energy availability.

retina | photoreceptor | metabolism | degeneration | fovea

The open transduction channels and associated depolarized dark resting-membrane potential of rod photoreceptors makes their utilization of energy high in darkness but considerably lower even in moderate background light (1, 2). Energy expenditure could be much higher for cones, which continue to respond in bright illumination and make many more synapses onto second-order retinal cells. In most mammals, cones represent only a small fraction of the total number of photoreceptors, making direct measurements of ATP turnover with biochemical techniques (3) or oxygen consumption (1) problematic. Instead, we have used recently available voltage-clamp recordings from mouse cones in retinal slices (4) to calculate the rate of ATP utilization of the most energy-intensive cellular functions of the photoreceptors.

We have characterized the light-sensitive conductance in the cone outer segment and voltage-gated conductances in the cone inner segment, and because ion transport is by far the greatest component of the energy balance of photoreceptors (2) and of neurons in the brain (5, 6), we can use these physiological measurements to estimate mammalian cone ATP expenditure compared with rods. Our calculations show that ATP is consumed at a much higher rate in single cones, even in dim light but especially in bright daylight. Because rods are so much more numerous than cones in most mammals, the total ATP consumption of rods still exceeds that of cones. In the primate retina, however, the high density of cones in the fovea produces a large increase in energy utilization in the center of the retina. Several recent publications have implicated glucose transport or availability in the degeneration of cones (7–10), and it is possible that this high cone ATP requirement has some role in the progression of cone loss. Our observations may help explain why foveas are so rare among mammals, and why degenerating cones first lose their outer segments, probably at least in part to decrease the load of entering Na^+.

Results and Discussion

To measure the light-dependent inward current of the cone outer segment, we recorded voltage-clamp current responses from both rods and cones in slices of mouse retina, using techniques described previously (*SI Appendix*) (4, 11, 12). We used mice lacking connexin-36 gap junctions ($Cx36^{-/-}$) to avoid any cross-contamination of rod and cone signals (13) and to achieve a more accurate space clamp of the cell. The light-dependent current is produced by Na^+ and Ca^{2+} ions, which enter through cyclic nucleotide-gated (CNG) channels and are subsequently removed by ATP-dependent transport of Na^+ via a Na^+/K^+ pump and by transport of Ca^{2+} by Na^+/K^+-Ca^{2+} (NCKX) exchange. From measurements of current responses (14), and from the voltages at corresponding light intensities (Fig. 1*B*), the reversal potential of the light response (4), and the current-voltage curve of the light-dependent conductance (4), we calculated the entry of Na^+ into the outer segment as the sum of the Na^+ entering the CNG channels plus the Na^+ entry required to export Ca^{2+} via the exchanger (*SI Appendix*) (2). We assumed that the exchanger current was 10% of the total current (15) and divided the net Na^+ entry by 3 to give the ATP consumed by the Na^+/K^+ ATPase. The exact value of the exchanger current has a relatively small effect on the total Na^+ entry that we calculated (Eq. **6** in *SI Appendix*); doubling its fraction from 10% to 20% increases the Na^+ influx by only 10%. Our calculation ignores the outward current carried by K^+ through the CNG channels, which would lead us to underestimate the value of the Na^+ influx. This effect is again small; we estimated this K^+ current to be approximately 14% of the total current in darkness (*SI Appendix*) and to decrease as the cone hyperpolarizes toward the K^+ equilibrium potential in the light.

We next considered ion influx through voltage-gated channels in the inner segment. Pumping of Ca^{2+} in the inner segment makes an important contribution to photoreceptor ATP utilization (2), because both rods and cones have resting inward Ca^{2+} currents (i_{Ca}) in darkness to support a continuous release of neurotransmitter (16). We routinely measured maximum values of i_{Ca} >50 pA in cones (Fig. 1*C*) (4); rod i_{Ca} was much smaller, with currents rarely exceeding 10 pA, consistent with the smaller size of the rod spherule

Significance

From recent measurements of mammalian cone physiology, we have calculated cone ATP utilization in darkness and in the light. We show that single cones consume ATP at a much higher rate than single rods, a difference that is greatly increased during the day. This high metabolic rate is especially prominent in the primate fovea, which may make this part of the human eye particularly sensitive to decreases in glucose uptake or other metabolic alterations.

Author contributions: N.T.I., G.L.F., and A.P.S. designed research; N.T.I. performed research; N.T.I., G.L.F., and A.P.S. analyzed data; and N.T.I., G.L.F., and A.P.S. wrote the paper.

The authors declare no competing interest.

This article is a PNAS Direct Submission.

[1]To whom correspondence may be addressed. Email: asampath@jsei.ucla.edu.

This article contains supporting information online at https://www.pnas.org/lookup/suppl/doi:10.1073/pnas.2001776117/-/DCSupplemental.

First published July 27, 2020.

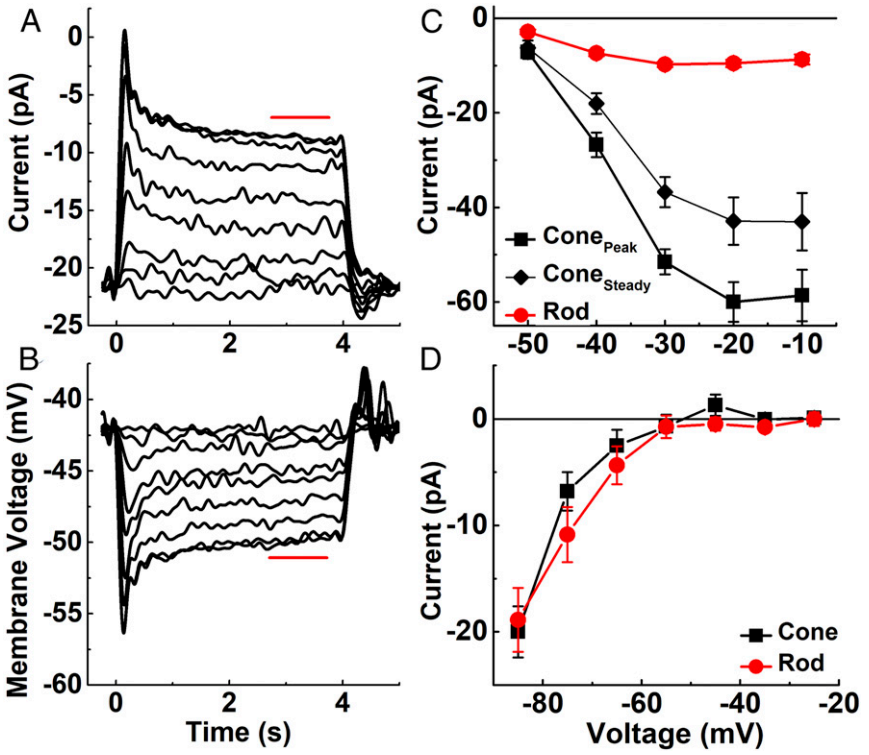

Fig. 1. Light responses and voltage-gated currents of mouse cones. (*A* and *B*) Cones from *Cx36*$^{-/-}$ retinas were illuminated with 4 s of steady 405-nm light at following intensities (in effective photons s^{-1} at the λ_{max} value of either the M or S cone pigment): 4.4×10^4, 2.1×10^5, 8.1×10^5, 2.3×10^6, 4.8×10^6, 9.6×10^6, 2.4×10^7, 4.8×10^7, 6.6×10^7. (*A*) Mean current responses from four cones held at a membrane potential of −50 mV. (*B*) Mean voltage responses from seven cones to the same light-intensity steps as in *A*. Red bars indicate region of responses averaged to calculate steady-state response. (*C*) Amplitude of Ca^{2+} current to depolarizing voltage steps in darkness, measured in the presence of 200 μm niflumic acid in the external perfusion solution to block Ca^{2+}-activated Cl^- currents (4). Photoreceptors were held at −70 mV and then stepped for 0.75 s to depolarizing potentials (−50 to 0 mV in 10-mV increments). Data show peak current and current measured just before termination of the voltage step ("steady") plotted against holding potential. Symbols are mean ± SEM values for 14 cones and 9 rods. The horizontal line indicates zero current. (*D*) Mean i_h current from 7 cones and 13 rods recorded as in Ingram et al. (4) by holding V_m at −30 mV and stepping for 400 ms to hyperpolarizing potentials (−25 mV to −85 mV in 10-mV increments). We included 25 mM tetraethylammonium and 10 μm isradipine in the external perfusion solution to block K^+ and Ca^{2+} currents. The horizontal line indicates zero current.

compared with the cone pedicle and the single glutamate release site made by rods onto rod bipolar cells and horizontal cells. After directly measuring the voltage dependence of the current for both photoreceptor types (Fig. 1*C*), the influx of Ca^{2+} was interpolated at each light-induced change in membrane potential (Fig. 1*B*). Ca^{2+} is extruded from the inner segment by a plasma membrane ATPase rather than by Na^+-dependent transport (17–19), so ATP utilization can be estimated simply by dividing Ca^{2+} influx by 2.

Entering Ca^{2+} gates a Ca^{2+}-activated Cl^- current, which can be almost as large in amplitude as the Ca^{2+} current (4). Because the mechanism of Cl^- transport is still unclear, no attempt was made to take it into consideration. As Fig. 1*C* shows, however, the Ca^{2+} current is much larger for cones than for rods, which should also be true of the Ca^{2+}-activated Cl^- current. Therefore, including any ATP required to transport Cl^- would only augment the difference between the two kinds of photoreceptors and would not change the main conclusions of this study.

Both rods and cones also have a mixed Na^+/K^+ conductance provided by hyperpolarization-activated cyclic nucleotide-gated (HCN) channels (16), which produce a current, i_h (4). The rod and cone currents have a similar voltage dependence (Fig. 1*D*), as expected based on their predominantly HCN1 composition (20–22). To calculate Na^+ entry through these channels (*SI Appendix*), we used cone voltage responses (Fig. 1*B*), the relative permeability of the channels for Na^+ (4), the ion concentration gradients, and the Goldman–Hodgkin–Katz current equation (23). This calculation also includes the energy required to pump back the K^+ leaving through HCN channels and other voltage-gated K^+ channels (16), since the Na^+/K^+ ATPase produces homeostasis of both Na^+ and K^+ at steady-state, in darkness or in steady light.

In addition to ion influx, the most important additional contributor to ATP utilization is likely to be synthesis of cGMP by guanylyl cyclase (2). The rate of the cyclase is modulated by the guanylyl-cyclase activating proteins (GCAPs), which increase the production of cGMP as the outer segment Ca^{2+} concentration declines during illumination. We assumed that the Ca^{2+} concentration in mouse cones is directly proportional to the current through the CNG channels, as previous experiments have shown to be true for salamander rods (24) and cones (25); and because rods and cones use similar cyclases and GCAPs, we estimated cyclase activity from the known rod maximum and minimum cyclase rates and the dependence of the rate on Ca^{2+} concentration (*SI Appendix*) (26). Since cyclase is likely to be more highly expressed in cones by as much as a factor of 10 (27), we increased cone values by this factor. Nevertheless, the contribution of the cyclase even after this adjustment was relatively small compared with that required for ion pumping. Consequently, even substantial alterations in the assumptions we have made in calculating the ATP required for cGMP synthesis would be unlikely to have a significant effect on the energy balance of the photoreceptor.

Fig. 2 summarizes the intensity dependence of ATP utilization in rods (Fig. 2*A*) and cones (Fig. 2*B*) due to the CNG channels,

HCN channels, Ca^{2+} extrusion, and cGMP production. From these components alone, cones require roughly 10^8 ATPs/s even in bright light (Fig. 2*B*). Contributions of pigment phosphorylation, synaptic vesicle synthesis, and protein synthesis are likely to be small in comparison. To phosphorylate bleached pigment, cones in mice use the same rhodopsin kinase (GRK1) as rods; this enzyme is expressed at a level of several percent of the pigment concentration and has a low turnover number (28). Even if all of the serines and threonines of each of the bleached pigment molecules were phosphorylated, which seems unlikely (29), the rate of ATP utilization would be unlikely to ever exceed 10^6 s^{-1}. Regeneration of pigment is also unlikely to require $>10^6$ ATPs/s (*SI Appendix*), particularly for cones, which reisomerize chromophore at least in part via a light-dependent mechanism (30).

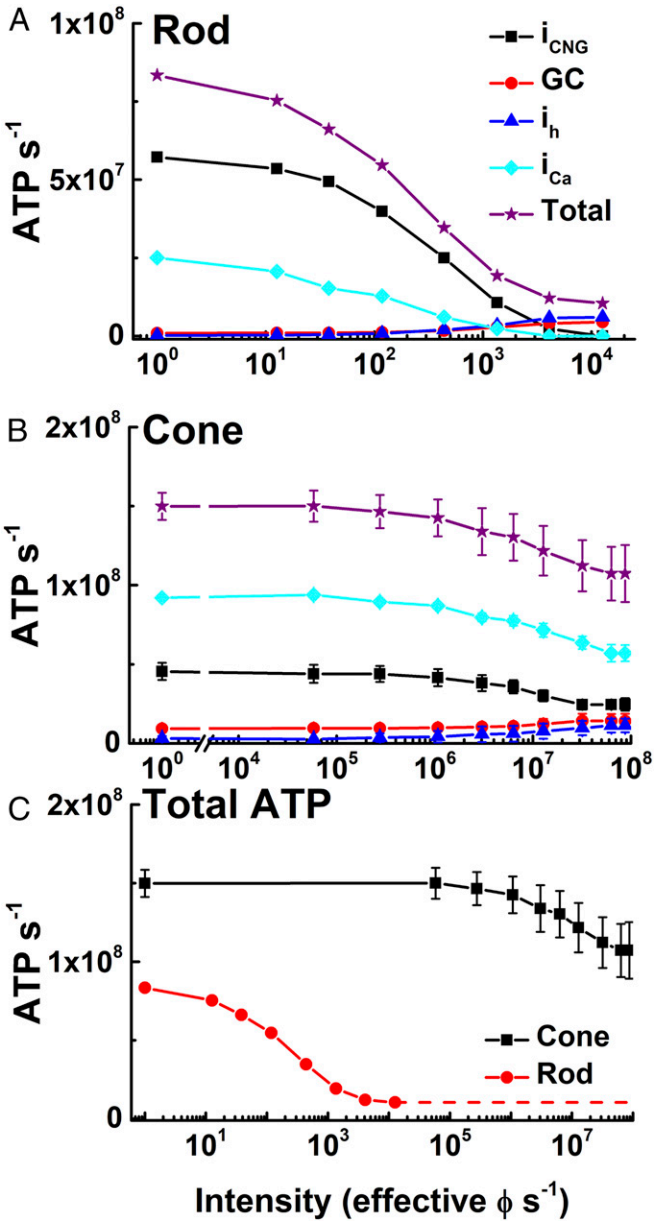

Fig. 2. ATP consumption in rods and cones in steady light. (*A* and *B*) Net ATP consumption for rods (*A*) and cones (*B*) as a function of light intensity in photons s^{-1}, effective at the λ_{max} of the rod or cone photopigments (*SI Appendix*). ATP consumption was then calculated from physiological measurements in Fig. 1 (*SI Appendix*), due to CNG channels (i_{CNG}, black squares), HCN channels (i_h, blue triangles), Ca^{2+} influx at synaptic terminals (i_{Ca}, cyan diamonds), guanylyl cyclase (GC, red circles), and sum of all four (total, purple stars). (*C*) Total ATP consumed for rods (red) and cones (black). Data are mean ± SEM.

Cones release synaptic transmitter in darkness at the rate of a few hundred vesicles per second (31), requiring on the order of 10^4 ATPs per vesicle (5, 6) for a total of ~2 to 3 × 10^6 ATPs/s in darkness, decreasing in the light. Protein synthesis to renew the components of outer-segment membrane would require the synthesis of ~10% of 10^8 protein molecules per outer segment per day, amounting to a few hundred protein molecules per second. Even including lipid synthesis, the ATP required to renew the outer segment is unlikely to be $>10^5$ s^{-1}, much less than ion transport. The pumping of ions into endoplasmic reticulum and other intracellular vesicles is also unlikely to require high rates of ATP turnover comparable to those shown in Fig. 2. To our knowledge, there is no evidence that ion transport across intracellular vesicles or membranes must be maintained in the presence of a large leak of ions, as in the inner and outer segments.

Fig. 2*C* compares our calculations of the total energy used by rods and cones. In rods, ATP is consumed largely to remove Na^+ from the outer segment and Ca^{2+} from the inner segment at a rate that is highest in darkness, decreasing precipitously even in moderate illumination as the rods approach saturation and nearly all of the CNG channels close. Because cones never saturate even in very bright light, they are much more expensive metabolically per cell. They use almost twofold more ATP in darkness because of the larger synaptic Ca^{2+} current, which in cones requires even more energy than removal of outer segment Na^+. In addition, because cones are less sensitive than rods and do not saturate, ATP utilization remains high over a substantial part of the range of vision and never drops to below ~10^8 ATPs/cone/s.

The consequence of this much higher energy requirement can be more clearly appreciated from the distribution of rods and cones in the retina. In mouse, rods greatly outnumber cones (32, 33) and consume much more ATP in darkness (Fig. 3*A*). As the ambient light intensity increases (Fig. 3 *B* and *C*), rod energy utilization decreases, but because rods are so much more abundant, they continue to consume more ATP than cones over the entire retina. This situation is dramatically different in primates, whose cones are physiologically quite similar to those of mouse (34, 35). Cones are again less numerous (36, 37) and less important consumers of ATP overall (Fig. 3*D*), but throughout most of the range of daily illumination, the high concentration of active cones in the very center of the retina produces a large and prominent peak of ATP consumption at the fovea (Fig. 3 *E* and *F*). Because the outer segments of primate cones are approximately three times longer than those of mouse cones (38, 39), they would be expected to have larger circulating currents and an even greater energy requirement than we have estimated. Humans, like most mammals, have many more rods than cones, but cluster cones together in the fovea to improve acuity at the center of gaze while keeping the total number of these more expensive cells to a minimum. This strategy reduces the overall consumption of ATP by the retina but has one disadvantage: it creates a small region with a particularly high energy requirement, which could make the fovea at especially high risk when glucose transport or availability is diminished (7–10).

Our observations may provide some explanation for why a fovea is so rare among mammals and other vertebrate species. The metabolic cost associated with maintaining a high density of cones at the center of the visual field would make sense only if there were a selective pressure for particularly high visual acuity and temporal resolution. The high metabolic cost may also help explain why cones in diseased retinas first lose their outer segments (41, 42) and can then remain viable for a very long time as rounded cell bodies (7). These "dormant" cones have been

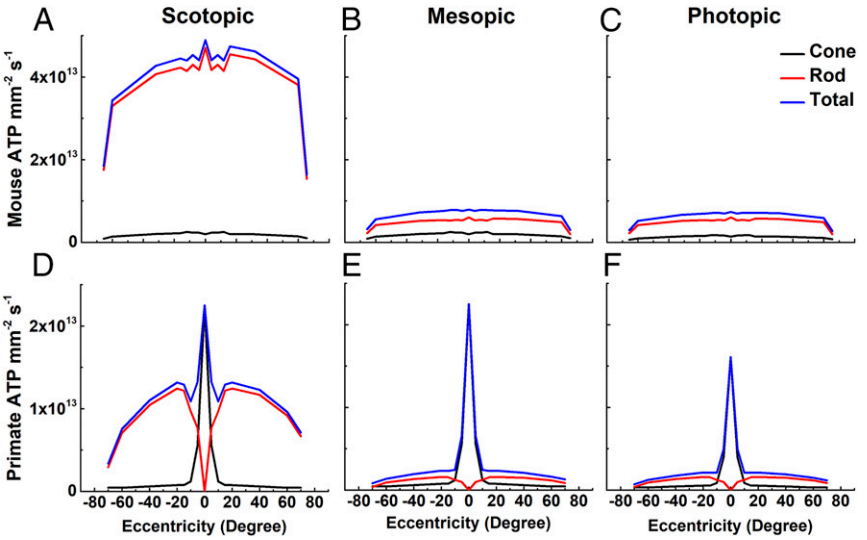

Fig. 3. ATP consumption across retinal eccentricities. We used total ATP consumption for rods and cones from Fig. 2 together with measurements of the density of photoreceptors as a function of retinal eccentricity (mouse, 32; human, 36) to calculate the metabolic demand of the outer retina in mouse (*A*–*C*) and human (*D*–*F*) in three ambient light intensities: scotopic (darkness; 0 effective ϕ cell^{-1}s^{-1}) (*A* and *D*); mesopic (12,600 effective ϕ rod^{-1}s^{-1} or 12,500 effective ϕ cone^{-1}s^{-1}) (*B* and *E*); and photopic (8.8×10^7 effective ϕ rod^{-1}s^{-1} or 8.7×10^7 effective ϕ cone^{-1}s^{-1}) (*C* and *F*). The same values were used for cone currents, even though foveal cone outer segments are three times longer than mouse cones (38, 39) and likely have larger circulating currents. No attempt was made to take the difference in the number of synaptic ribbons in the pedicles between foveal and peripheral cones into consideration (40); these factors would only increase the difference in ATP consumption between rods and cones.

proposed as potential targets for clinical intervention (9, 43). It is widely surmised that cones lose their outer segments to spare the energy to reform them. We think it more likely that outer segments are lost to prevent Na^+ load from entry through CNG channels. An increase in intracellular Na^+ can produce an increase in Ca^{2+}, because the decrease in the Na^+ gradient produces a decrease in Ca^{2+} export via NCKX exchange (44); an increase in Ca^{2+} in photoreceptors as in other cells can trigger apoptosis (45).

Materials and Methods

All experiments were performed in accordance with the rules and regulations of the NIH guidelines for research animals, as approved by the Institutional Animal Care and Use Committee of the University of California Los Angeles. Mice were kept under cyclic light (12-h on/12-h off) with ad libitum food and water in approved cages. Male and female mice were used in approximately equal numbers and were between 2 and 6 mo of age. To limit both the contribution of rod signals to cone responses and the spread of signal from a recorded cone, we recorded from mice that lacked the gap-junction protein connexin 36 (12). *Cx36*$^{-/-}$ mice were generated by David Paul from Harvard University (46) and obtained from Sam Wu of the Baylor College of Medicine. Rods and cones were voltage-clamped in dark-adapted retinal slices. Methods of recording and calculations of ATP turnover were similar to those described in our previous publications (2, 4, 11, 12). A more detailed description is given in the *SI Appendix*.

Data Availability. All the data in the paper are given in the figures except for the traces in Fig. 1 *A* and *B*. The data for these traces have been deposited and are available in University of California, Los Angeles (UCLA) Dataverse (https://dataverse.ucla.edu/dataset.xhtml?persistentId=doi:10.25346/S6/R3JVO2).

ACKNOWLEDGMENTS. We thank Rikard Frederiksen and Jürgen Reingruber for helpful discussions, Greg Field for comments on an earlier draft of the manuscript, and Ekaterina Bikovtseva for technical assistance. This work was supported by National Eye Institute (NEI) Grant R01 EY001844 (to G.L.F.), T32 EY07026 (to A.P.S.), and R01 EY29817 (to A.P.S.); a Dissertation-Year Fellowship from the Graduate Division of UCLA (to N.T.I.); an unrestricted grant from Research to Prevent Blindness USA to the UCLA Department of Ophthalmology; and NEI Core Grant EY00311 to the Jules Stein Eye Institute.

1. R. A. Linsenmeier, R. D. Braun, Oxygen distribution and consumption in the cat retina during normoxia and hypoxemia. *J. Gen. Physiol.* **99**, 177–197 (1992).
2. H. Okawa, A. P. Sampath, S. B. Laughlin, G. L. Fain, ATP consumption by mammalian rod photoreceptors in darkness and in light. *Curr. Biol.* **18**, 1917–1921 (2008).
3. S. M. Dawis *et al*., Adenosine triphosphate utilization rates and metabolic pool sizes in intact cells measured by transfer of ^{18}O from water. *Biophys. J.* **55**, 79–99 (1989).
4. N. T. Ingram, A. P. Sampath, G. L. Fain, Membrane conductances of mouse cone photoreceptors. *J. Gen. Physiol.* **152**, e201912520 (2020).
5. D. Attwell, S. B. Laughlin, An energy budget for signaling in the grey matter of the brain. *J. Cereb. Blood Flow Metab.* **21**, 1133–1145 (2001).
6. P. Sterling, S. Laughlin, *Principles of Neural Design*, (MIT Press, Cambridge, MA, 2015).
7. C. Punzo, K. Kornacker, C. L. Cepko, Stimulation of the insulin/mTOR pathway delays cone death in a mouse model of retinitis pigmentosa. *Nat. Neurosci.* **12**, 44–52 (2009).
8. N. Aït-Ali *et al*., Rod-derived cone viability factor promotes cone survival by stimulating aerobic glycolysis. *Cell* **161**, 817–832 (2015).
9. W. Wang *et al*., Two-step reactivation of dormant cones in retinitis pigmentosa. *Cell Rep.* **15**, 372–385 (2016).
10. S. Y. Cheng *et al*., Altered photoreceptor metabolism in mouse causes late-stage age-related macular degeneration-like pathologies. *Proc. Natl. Acad. Sci. U.S.A.* **117**, 13094–13104 (2020).
11. J. Pahlberg *et al*., Voltage-sensitive conductances increase the sensitivity of rod photoresponses following pigment bleaching. *J. Physiol.* **595**, 3459–3469 (2017).
12. N. T. Ingram, A. P. Sampath, G. L. Fain, Voltage-clamp recordings of light responses from wild-type and mutant mouse cone photoreceptors. *J. Gen. Physiol.* **151**, 1287–1299 (2019).
13. G. L. Fain, A. P. Sampath, Rod and cone interactions in the retina. *F1000Res.* **7**, 657 (2018).
14. N. T. Ingram, G. L. Fain, A. P. Sampath, Step responses mouse Cx36$^{-/-}$ cones, UCLA Dataverse. https://doi.org/10.25346/S6/R3JVO2. Deposited 3 June 2020.
15. R. J. Perry, P. A. McNaughton, Response properties of cones from the retina of the tiger salamander. *J. Physiol.* **433**, 561–587 (1991).
16. M. J. Van Hook, S. Nawy, W. B. Thoreson, Voltage- and calcium-gated ion channels of neurons in the vertebrate retina. *Prog. Retin. Eye Res.* **72**, 100760 (2019).
17. D. Krizaj, D. R. Copenhagen, Compartmentalization of calcium extrusion mechanisms in the outer and inner segments of photoreceptors. *Neuron* **21**, 249–256 (1998).
18. C. W. Morgans, O. El Far, A. Berntson, H. Wässle, W. R. Taylor, Calcium extrusion from mammalian photoreceptor terminals. *J. Neurosci.* **18**, 2467–2474 (1998).
19. D. Cia *et al*., Voltage-gated channels and calcium homeostasis in mammalian rod photoreceptors. *J. Neurophysiol.* **93**, 1468–1475 (2005).
20. S. Moosmang *et al*., Cellular expression and functional characterization of four hyperpolarization-activated pacemaker channels in cardiac and neuronal tissues. *Eur. J. Biochem.* **268**, 1646–1652 (2001).
21. F. Müller *et al*., HCN channels are expressed differentially in retinal bipolar cells and concentrated at synaptic terminals. *Eur. J. Neurosci.* **17**, 2084–2096 (2003).

22. G. C. Knop *et al*., Light responses in the mouse retina are prolonged upon targeted deletion of the HCN1 channel gene. *Eur. J. Neurosci.* **28**, 2221–2230 (2008).
23. A. L. Hodgkin, B. Katz, The effect of sodium ions on the electrical activity of giant axon of the squid. *J. Physiol.* **108**, 37–77 (1949).
24. H. R. Matthews, G. L. Fain, The effect of light on outer segment calcium in salamander rods. *J. Physiol.* **552**, 763–776 (2003).
25. A. P. Sampath, H. R. Matthews, M. C. Cornwall, J. Bandarchi, G. L. Fain, Light-dependent changes in outer segment free-Ca^{2+} concentration in salamander cone photoreceptors. *J. Gen. Physiol.* **113**, 267–277 (1999).
26. E. V. Olshevskaya *et al*., The Y99C mutation in guanylyl cyclase-activating protein 1 increases intracellular Ca^{2+} and causes photoreceptor degeneration in transgenic mice. *J. Neurosci.* **24**, 6078–6085 (2004).
27. N. Takemoto, S. Tachibanaki, S. Kawamura, High cGMP synthetic activity in carp cones. *Proc. Natl. Acad. Sci. U.S.A.* **106**, 11788–11793 (2009).
28. M. J. Kennedy *et al*., Multiple phosphorylation of rhodopsin and the in vivo chemistry underlying rod photoreceptor dark adaptation. *Neuron* **31**, 87–101 (2001).
29. S. A. Vishnivetskiy *et al*., Regulation of arrestin binding by rhodopsin phosphorylation level. *J. Biol. Chem.* **282**, 32075–32083 (2007).
30. A. Morshedian *et al*., Light-driven regeneration of cone visual pigments through a mechanism involving RGR opsin in Muller Glial cells. *Neuron* **102**, 1172–1183.e5 (2019).
31. S. Y. Choi *et al*., Encoding light intensity by the cone photoreceptor synapse. *Neuron* **48**, 555–562 (2005).
32. C.-J. Jeon, E. Strettoi, R. H. Masland, The major cell populations of the mouse retina. *J. Neurosci.* **18**, 8936–8946 (1998).
33. S. Volland, J. Esteve-Rudd, J. Hoo, C. Yee, D. S. Williams, A comparison of some organizational characteristics of the mouse central retina and the human macula. *PLoS One* **10**, e0125631 (2015).
34. T. Yagi, P. R. Macleish, Ionic conductances of monkey solitary cone inner segments. *J. Neurophysiol.* **71**, 656–665 (1994).
35. J. Baudin, J. M. Angueyra, R. Sinha, F. Rieke, S-cone photoreceptors in the primate retina are functionally distinct from L and M cones. *eLife* **8**, e39166 (2019).
36. C. A. Curcio, K. R. Sloan Jr., O. Packer, A. E. Hendrickson, R. E. Kalina, Distribution of cones in human and monkey retina: Individual variability and radial asymmetry. *Science* **236**, 579–582 (1987).
37. G. Østerberg, Topography of the layer of rods and cones in the human retina. *Acta Opthalmologica (Copenhagen)* (suppl. 6), 1–103 (1935).
38. J. E. Dowling, Foveal receptors of the monkey retina: Fine structure. *Science* **147**, 57–59 (1965).
39. L. D. Carter-Dawson, M. M. LaVail, Rods and cones in the mouse retina. I. Structural analysis using light and electron microscopy. *J. Comp. Neurol.* **188**, 245–262 (1979).
40. M. H. Chun, U. Grünert, P. R. Martin, H. Wässle, The synaptic complex of cones in the fovea and in the periphery of the macaque monkey retina. *Vision Res.* **36**, 3383–3395 (1996).
41. I. Barone, E. Novelli, E. Strettoi, Long-term preservation of cone photoreceptors and visual acuity in rd10 mutant mice exposed to continuous environmental enrichment. *Mol. Vis.* **20**, 1545–1556 (2014).
42. B. Lin, R. H. Masland, E. Strettoi, Remodeling of cone photoreceptor cells after rod degeneration in rd mice. *Exp. Eye Res.* **88**, 589–599 (2009).
43. V. Busskamp *et al*., Genetic reactivation of cone photoreceptors restores visual responses in retinitis pigmentosa. *Science* **329**, 413–417 (2010).
44. L. Cervetto, L. Lagnado, R. J. Perry, D. W. Robinson, P. A. McNaughton, Extrusion of calcium from rod outer segments is driven by both sodium and potassium gradients. *Nature* **337**, 740–743 (1989).
45. M. Power *et al*., Cellular mechanisms of hereditary photoreceptor degeneration—Focus on cGMP. *Prog. Retin. Eye Res.* **74**, 100772 (2019).
46. M. R. Deans, B. Volgyi, D. A. Goodenough, S. A. Bloomfield, D. L. Paul, Connexin36 is essential for transmission of rod-mediated visual signals in the mammalian retina. *Neuron* **36**, 703–712 (2002).